BIOCHEMISTRY
including biophysical chemistry & molecular biology
Article

Biochemistry **2009,** *48,* 9287–9296 9287
DOI: 10.1021/bi900852m

Effects of Phospholamban Transmembrane Mutants on the Calcium Affinity, Maximal Activity, and Cooperativity of the Sarcoplasmic Reticulum Calcium Pump†

Catharine A. Trieber, Michael Afara, and Howard S. Young*

Department of Biochemistry and National Institute for Nanotechnology, University of Alberta, Edmonton, Alberta T6G 2H7, Canada

Received May 19, 2009; Revised Manuscript Received August 21, 2009

ABSTRACT: Regulation of the SERCA calcium pump by phospholamban (PLB) is largely due to interactions between their respective transmembrane domains. In spite of numerous mutagenesis and kinetic studies, we still do not have a clear mechanistic picture of how PLB influences the calcium transport cycle of SERCA. Herein, we have created alanine mutants for each residue in the transmembrane domain of PLB, we have co-reconstituted these mutants with SERCA into proteoliposomes, and we have performed kinetic simulations of the calcium-dependent ATPase activity isotherms. The PLB transmembrane mutants had a variable effect on the calcium affinity, maximal activity, and cooperativity of SERCA, such that a range of values was observed. Kinetic simulations using a well-established reaction scheme for SERCA then allowed us to correlate the effects on SERCA activity with changes in the reaction scheme rate constants. Only three steps in the reaction scheme were affected by the presence of PLB, namely, binding of the first calcium ion, a subsequent conformational change in SERCA, and binding of the second calcium ion. The ability of wild-type and mutant forms of PLB to alter the apparent calcium affinity of SERCA correlated with a decreased rate of binding of the second calcium ion. In addition, the ability of wild-type and mutant forms of PLB to alter the maximal activity of SERCA correlated with a change in the forward rate constant for the slow conformational change in SERCA following binding of the first calcium ion.

In heart muscle, regulation of the sarcoplasmic reticulum (SR)[1] calcium pump (also known as Ca^{2+}-ATPase or SERCA) allows for a dynamic contraction−relaxation cycle. This cycle relies on the release, re-uptake, and maintenance of SR calcium stores in a process that is linked to the β-adrenergic pathway. Under the control of β-adrenergic stimulation, a second protein called phospholamban (PLB) directly interacts with SERCA and decreases its apparent affinity for calcium (*1*). PLB is a 52-amino acid integral membrane protein that is reversibly phosphorylated at Ser^{16} or Thr^{17} as a means of controlling the inhibitory interaction with SERCA. Depending on its phosphorylation state, PLB alters the calcium transport properties of SERCA, thereby allowing dynamic changes in the rate of calcium uptake and the overall calcium load in the SR. In turn, this determines the rate of muscle relaxation and the force of contraction.

It is generally accepted that SERCA inhibition by PLB is due to intramembrane interactions (*2*). The inhibitory capacity of PLB is encoded by the amino acid sequence and tertiary structure of its transmembrane domain, while the cytoplasmic domain mainly provides a means for reversibility of inhibition via phosphorylation. Extensive mutagenesis of both PLB and SERCA has led to a detailed description of the residues that contribute to the inhibitory interaction in terms of the consequences of mutation on the ability of PLB to alter the apparent calcium affinity of SERCA (*3*−*9*). Such studies have identified two functional regions on opposite faces of PLB's transmembrane helix: one region responsible for SERCA inhibition and the other region responsible for self-association. Mutations in the transmembrane domain of PLB that disrupt pentamer formation lead to superinhibition of SERCA, the so-called "mass action" theory (*5*). However, it was later recognized that residues distributed around most of PLB's transmembrane helix contribute to the interaction with SERCA, including residues in the leucine-isoleucine zipper (*8*). Such biochemical data combined with recent cross-linking studies (*10*−*14*) have provided the constraints necessary for molecular modeling of the inhibitory complex (*10*, *13*, *15*).

Despite this wealth of information, the biochemical data and molecular models describing the inhibitory complex of SERCA and PLB have not been completely reconciled with the kinetic description for calcium transport by SERCA (*16*, *17*). In the reaction scheme for calcium transport, calcium binding was postulated to involve three distinct steps (*16*), namely, binding of the first calcium ion, a conformational change that establishes cooperativity, and binding of the second calcium ion (Figure 1). A recent study by Mahaney and co-workers (*18*) postulated that PLB stabilizes a distinct E2-like calcium-free state of SERCA, thereby altering the transition to the E1 calcium-bound state. This concept is similar to the original description by Inesi and colleagues (*17*), who postulated that PLB alters the slow conformational change in SERCA following binding of the first calcium ion. Our studies with peptide mimics of PLB support this conclusion (*19*).

†This work was supported by grants from the Canadian Institutes of Health Research (MOP53306), the Canada Foundation for Innovation, and the Alberta Science and Research Investments Program. H.S.Y. is a Senior Scholar of the Alberta Heritage Foundation for Medical Research.

*To whom correspondence should be addressed. Phone: (780) 492-3931. Fax: (780) 492-0095. E-mail: hyoung@ualberta.ca.

[1]Abbreviations: TEV protease, tobacco etch virus protease; $C_{12}E_8$, octaethylene glycol monododecyl ether; EYPA, egg yolk phosphatidic acid; EYPC, egg yolk phosphatidylcholine; K_{Ca}, calcium concentration at half-maximal activity; MBP, maltose binding protein; n_H, Hill coefficient; OG, *n*-octyl glucoside; PLB, phospholamban; SERCA, sarco(endo)plasmic reticulum Ca^{2+}-ATPase; SR, sarcoplasmic reticulum; V_{max}, maximal activity.

Published on Web 08/26/2009

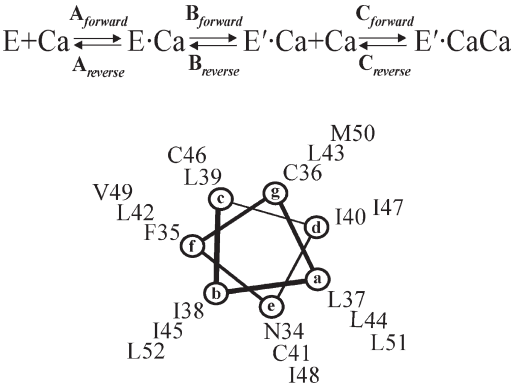

FIGURE 1: Part of the reaction scheme (top) for calcium transport by SERCA. Calcium binding involves three distinct steps, binding of the first calcium ion, a conformational change that establishes cooperativity, and binding of the second calcium ion. Helical wheel diagram (bottom) of PLB showing transmembrane residues 34−52. These residues of PLB were mutated to alanine in this study.

In this study, we have tested this hypothesis using co-reconstituted proteoliposomes (*20*). Starting with recombinant PLB (*21*), we have created alanine mutants for each residue of the transmembrane (TM) domain (residues 34−52). These recombinant PLB mutants were co-reconstituted with skeletal muscle SERCA into proteoliposomes, and the effects on the calcium-dependent ATPase activity of SERCA were determined (*20*). Each mutant had a distinct effect on the calcium affinity, maximal activity, and cooperativity of SERCA, such that a range of values was observed. Using a well-established reaction scheme for SERCA (*16*, *17*), kinetic simulation of the ATPase activity isotherms in the presence of the PLB mutants allowed us to compare the effects on SERCA activity with changes in the reaction rate constants for calcium binding (*19*, *22*). To summarize our results, we found that the effects of PLB on the calcium affinity, maximal activity, and cooperativity of SERCA were readily explained by changes to specific rate constants in the reaction scheme for calcium binding. First, PLB altered the slow conformational change in SERCA following binding of the first calcium ion, consistent with previous observations (*17*−*19*). However, PLB also lowered the forward rate constant for binding of the second calcium ion, and it was this latter behavior that correlated with the effects on the apparent calcium affinity of SERCA. Second, this observation was supported by a relationship between this same forward rate constant and the apparent cooperativity of SERCA. Third, the ability of PLB to increase the maximal activity of SERCA correlated with the forward rate constant for the slow conformational change in SERCA following binding of the first calcium ion. While the majority of the PLB mutants followed these general trends, several mutants deviated from this behavior (Leu^{37}, Leu^{39}, Cys^{46}, and Ile^{47}), and these mutants are discussed in detail below.

EXPERIMENTAL PROCEDURES

Materials. Octaethylene glycol monododecyl ether ($C_{12}E_8$) was obtained from Barnet Products (Englewood Cliff, NJ). SM-2 Biobeads were obtained from Bio-Rad (Hercules, CA). Egg yolk phosphatidylcholine (EYPC) and egg yolk phosphatidic acid (EYPA) were obtained from Avanti Polar Lipids (Alabaster, AL). *n*-Octyl glucopyranoside (OG) was obtained from Anatrace (Maumee, OH). All reagents for the coupled enzyme assay (*23*) for measuring calcium-dependent ATPase activity were of the highest available purity (Sigma-Aldrich, Oakville, ON). EZ-Link Sulfo-NHS-LC-Biotin (sulfosuccinimidyl-6-[biotin-amido]hexanoate) was obtained from Thermo Scientific (Rockford, IL). IRDye 800CW streptavidin conjugate and Odyssey Blocking Buffer were obtained from LI-COR Bioscience (Lincoln, NE). Amylose resin was purchased from New England Biolabs (Pickering, ON).

Mutagenesis and Expression of Recombinant PLB. Recombinant PLB was expressed and purified from bacterial cell culture as described previously (*20*, *21*). Briefly, all mutants were constructed from the human wild-type PLB gene cloned into the pMal-c2x plasmid to generate a maltose binding protein (MBP) fusion protein with a TEV protease cleavage site between MBP and PLB. After site-directed PCR mutagenesis, the PCR products were cloned into the pM-PLB plasmid, replacing the wild-type gene, and confirmed by sequencing (DNA Core Facility, University of Alberta). The individual mutants were expressed in *Escherichia coli* DH5α cells. Briefly, an overnight 50 mL starter culture was diluted into 1 L of LB medium supplemented with 0.2% glucose and 50 μg/mL ampicillin. The culture was induced with 100 μM IPTG and incubated at 22 °C for 22 h. Cells were collected by centrifugation, transferred into lysis buffer [20 mM phosphate (pH 8.0), 120 mM NaCl, 1 mM EDTA, 0.5% glycerol, 0.5% Triton X-100, 0.1 mM dithiothreitol, 0.5 mM phenylmethanesulfonyl fluoride, 2 μg/mL pepstatin A, and 2 μg/mL leupeptin], and disrupted by sonication. After centrifugation to remove cellular debris, the supernatant containing the MBP fusion protein was purified by amylose affinity chromatography and cleaved with TEV protease. Finally, PLB was purified to homogeneity by selective solubilization in guanidine hydrochloride followed by reverse-phase high-performance liquid chromatography.

Co-Reconstitution of SERCA and Recombinant PLB. Following established procedures, rabbit skeletal muscle SERCA was purified from SR vesicles (*24*) by affinity chromatography (*25*). Functional co-reconstitution of SERCA with PLB has also been described in detail (*20*, *21*, *26*−*29*). Typically, 100 μg of PLB in 80% 2-propanol was mixed with lipids (360 μg of EYPC and 40 μg of EYPA), dried to a thin film under nitrogen gas, and evaporated under high vacuum to remove residual solvents. The PLB and lipid mixture was rehydrated in water for 15 min at 50 °C. Detergent (800 μg of $C_{12}E_8$) was added followed by vigorous vortexing to solubilize the mixture, followed by the addition of buffer [20 mM imidazole (pH 7.0), 100 mM KCl, and 0.02% NaN_3]. SERCA (300 μg) was added to this mixture to achieve final molar stoichiometries of 1 SERCA, 6 PLB, and 195 lipids. The co-reconstituted proteoliposomes containing SERCA and PLB were formed by the slow removal of detergent (with SM-2 Biobeads) followed by purification on a sucrose step gradient (*20*, *27*). The purified co-reconstituted proteoliposomes typically yield final molar stoichiometries of 1 SERCA, 4.5 PLB, and 120 lipids (*20*).

Orientation of PLB in Co-Reconstituted Proteoliposomes. The orientation of PLB in our co-reconstituted proteoliposomes was determined using a biotin surface labeling assay. Co-reconstituted vesicles (~5 μg of protein) were mixed in labeling buffer [20 mM borate-KOH (pH 9.0)] with 5 mM EZ-Link Sulfo-NHS-LC-Biotin in the absence and presence of 0.5% OG. The mixture was incubated at 4 °C for 2 h followed by quenching with an equal volume of SDS−PAGE sample buffer. After SDS−PAGE and electroblotting to Immobilon-FL PVDF membranes (Millipore, Bedford, MA), the amount of biotin labeling was quantified using IRDye 800CW streptavidin

conjugate and an Odyssey Infrared Imaging System (LI-COR Bioscience).

Activity Assays. Calcium-dependent ATPase activities of the co-reconstituted proteoliposomes were measured by a coupled enzyme assay (*23*). All co-reconstituted PLB mutants were compared to a negative control (SERCA reconstituted in the absence of PLB) and a positive control (SERCA co-reconstituted in the presence of wild-type PLB). A minimum of three independent reconstitutions and activity assays were performed for each PLB mutant, and the calcium-dependent ATPase activity was measured over a wide range of calcium concentrations (from 0.1 to 10 μM) for each. This method has been described in detail previously (*20*, *21*). The K_{Ca} (calcium concentration at half-maximal activity), the V_{max} (maximal activity), and the n_H (Hill coefficient) were calculated on the basis of nonlinear least-squares fitting of the activity data to the Hill equation using Sigma Plot (SPSS Inc., Chicago, IL). Errors were calculated as the standard error of the mean for a minimum of four independent measurements. Comparison of K_{Ca}, V_{max}, and n_H parameters was conducted using ANOVA (between subjects, one-way analysis of variance) followed by the Holm−Sidak test for pairwise comparisons (Sigma Plot).

Kinetic Simulations. Reaction rate simulations have been described for the transport cycle of SERCA in the absence and presence of PLB inhibition (*17*), and we have adopted this approach to understand SERCA inhibition by peptide mimics of PLB (*19*, *22*). In this study, we performed a global nonlinear regression fit of the model of Cantilina et al. (*17*) to each plot of SERCA ATPase activity versus calcium concentration using Dynafit [Biokin Inc., Pullman, WA (*30*)]. Such fits were performed for all co-reconstituted PLB mutants, which were compared to our control samples (SERCA reconstituted in the absence and presence of wild-type PLB). While all reaction rate constants were allowed to vary in the kinetic simulations, SERCA activities in the presence of PLB mutants were best fit with modifications to only three steps in the reaction cycle (Figure 1): (i) the binding of the first Ca^{2+} ion ($A_{forward}$), (ii) the slow isometric transition following the binding of the first Ca^{2+} ion ($B_{reverse}$), and (iii) binding of the second calcium ion ($C_{forward}$).

RESULTS

Via comparison of cardiac and skeletal muscle SR vesicles, it was initially shown that PLB inhibits SERCA by specifically increasing the activation energy for a calcium-induced conformational change in SERCA [by increasing $B_{reverse}$ (Figure 1)] (*17*). Later studies used scanning alanine mutagenesis of PLB in coexpression systems with SERCA to provide valuable insight into the regulatory role of PLB's transmembrane domain (*5*, *7*, *9*). From one point of view, we have a detailed kinetic description of the mode of PLB inhibition of SERCA. From another point of view, we have a thorough understanding of how individual residues of PLB contribute to SERCA inhibition. To bridge the gap between these two observations, more recent studies have attempted to link the effects of PLB mutants to particular reaction steps in the SERCA calcium transport cycle (*18*, *19*). Toward this goal, we have individually mutated all residues in the transmembrane domain of PLB to alanine (residues 34−52), and we have co-reconstituted each PLB mutant with SERCA into proteoliposomes. The measured calcium affinity, maximal activity, and cooperativity (n_H) of SERCA in the proteoliposomes were indicative of the functional effects of each PLB mutant. These measurements were then used in kinetic simulations aimed at understanding the mechanism by which PLB alters the calcium transport properties of SERCA.

Table 1: Maximal Activities, Apparent Calcium Affinities, and Hill Coefficients Determined for SERCA in the Absence and Presence of Wild-Type and Mutant Forms of PLB

	V_{max} (μmol mg^{-1} min^{-1})	K_{Ca} (μM)	n_H	n
SERCA	4.3 ± 0.1	0.41 ± 0.01	1.6 ± 0.1	28
PLB	6.0 ± 0.1	0.69 ± 0.01	2.0 ± 0.1	9
N34A	4.6 ± 0.1	0.45 ± 0.02	2.3 ± 0.2	6
F35A	5.2 ± 0.1	0.74 ± 0.04	1.7 ± 0.1	7
C36A	5.4 ± 0.2	0.97 ± 0.06	1.9 ± 0.2	9
L37A	4.0 ± 0.1	1.57 ± 0.04	1.9 ± 0.1	7
I38A	5.5 ± 0.1	0.49 ± 0.02	1.9 ± 0.1	6
L39A	5.2 ± 0.2	0.93 ± 0.07	1.7 ± 0.2	5
I40A	5.9 ± 0.1	0.91 ± 0.03	2.4 ± 0.1	8
C41A	5.8 ± 0.2	0.83 ± 0.05	1.9 ± 0.2	5
L42A	5.2 ± 0.1	0.58 ± 0.02	1.8 ± 0.1	7
L43A	6.0 ± 0.1	1.22 ± 0.05	1.9 ± 0.1	9
L44A	5.9 ± 0.1	1.11 ± 0.02	1.9 ± 0.1	9
I45A	5.1 ± 0.1	0.60 ± 0.03	2.1 ± 0.2	6
C46A	5.5 ± 0.1	0.66 ± 0.04	1.6 ± 0.1	6
I47A	5.4 ± 0.1	1.87 ± 0.07	1.9 ± 0.1	5
I48A	5.2 ± 0.1	0.69 ± 0.02	1.9 ± 0.1	6
V49A	5.3 ± 0.1	0.89 ± 0.05	1.8 ± 0.1	7
M50A	4.8 ± 0.1	0.62 ± 0.02	1.9 ± 0.1	8
L51A	4.5 ± 0.1	1.00 ± 0.07	1.9 ± 0.1	4
L52A	5.2 ± 0.1	0.65 ± 0.04	1.9 ± 0.2	5

Co-Reconstituted Proteoliposomes. Co-reconstitution at low lipid:protein ratios has provided a useful tool for the structural (*29*, *31*) and functional (*19*−*22*, *27*−*29*) characterization of the inhibitory complex of SERCA and PLB. Typically, the measurement of ATP hydrolysis rates by reconstituted SERCA proteoliposomes yielded a K_{Ca} of 0.41 μM, a V_{max} of 4.3 ± 0.1 μmol mg^{-1} min^{-1}, and a Hill coefficient indicative of cooperative calcium binding (Table 1). In the presence of wild-type PLB, the measurement of ATP hydrolysis rates by co-reconstituted proteoliposomes yielded a K_{Ca} of 0.69 μM, a V_{max} of 6.0 ± 0.1 μmol mg^{-1} min^{-1}, and a Hill coefficient indicative of increased cooperativity. The utility of these co-reconstituted proteoliposomes has been well documented (*19*−*22*, *27*−*29*, *31*, *32*), and our goal is not to reiterate their complete characteristics here. Nonetheless, the proteoliposomes have several properties that are critical for the experiments described below. First, the co-reconstituted proteoliposomes containing SERCA and PLB are tightly sealed such that they are impermeable to calcium, necessitating the use of a calcium ionophore for the ATPase activity measurements (*20*, *23*). Second, SERCA reconstitutes asymmetrically into the proteoliposomes such that all molecules are oriented with their cytoplasmic domains on the outer surface of the vesicles (*27*).

While the orientation of SERCA in the proteoliposomes is known, the orientation of PLB in the co-reconstituted proteoliposomes has not been determined. We have now used a biotin labeling strategy to determine the orientation of all PLB molecules within the proteoliposomes. A membrane-impermeable succinimidyl ester derivative of biotin, EZ-Link Sulfo-NHS-LC-Biotin, was used to specifically label Lys^3 and Lys^{27} of PLB. In the absence of detergent, molecules with their cytoplasmic domains on the outer surface of the proteoliposomes were labeled with biotin, while those facing the interior of the proteoliposomes

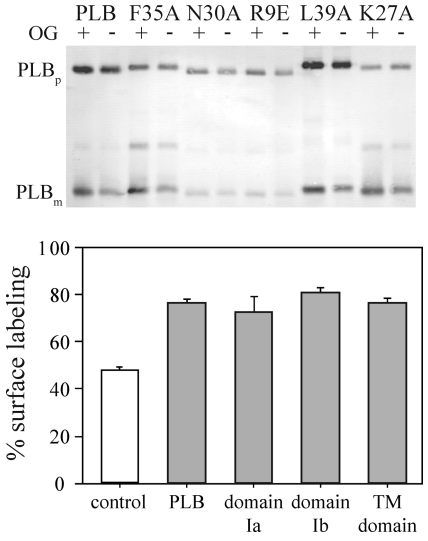

FIGURE 2: Biotin labeling and sidedness of PLB in the co-reconstituted proteoliposomes. The top panel shows a typical blot probed with IRDye 800CW streptavidin conjugate to detect biotin-labeled PLB in the absence and presence of detergent (*n*-octyl glucopyranoside). The wild type and several mutants of PLB representing all three structural domain are shown: domain 1a (R9E), domain 1b (K27A, N30A), and the transmembrane domain (F35A, L39A). The PLB pentamer (PLB_p) and monomer (PLB_m) are indicated. The bottom panel shows the quantitation of labeling for all wild-type and mutant PLB (*PLB*) or alanine mutants grouped according to domain (gray bars). On average, 78 ± 1% of the PLB molecules are correctly oriented with their cytoplasmic domains on the exterior surface of the co-reconstituted proteoliposomes. The white control bar shows the average biotin labeling of transmembrane peptides Leu_9 and Leu_{12} (*22*) co-reconstituted with SERCA into proteoliposomes.

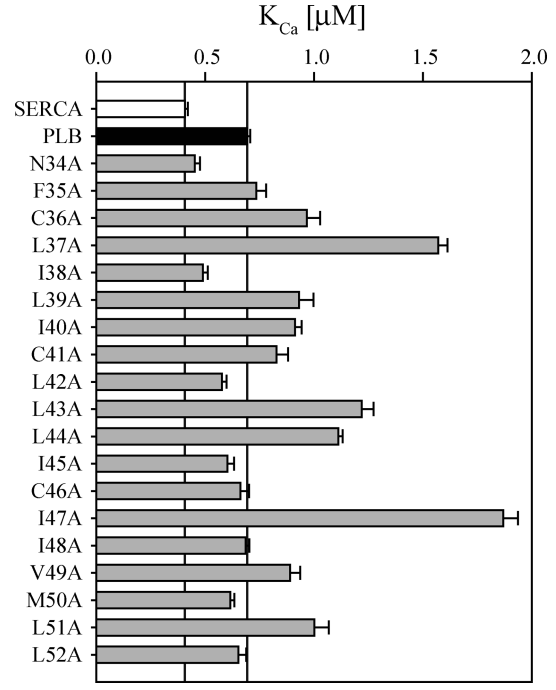

FIGURE 3: Effects of alanine mutation in the TM domain of PLB on the apparent calcium affinity (K_{Ca}) of SERCA. The vertical line at the left represents the K_{Ca} for SERCA reconstituted alone (white bar, $K_{Ca} = 0.41 \pm 0.01$ μM), and the vertical line at the right represents the K_{Ca} for SERCA co-reconstituted in the presence of wild-type PLB (black bar, $K_{Ca} = 0.69 \pm 0.01$ μM). The K_{Ca} values are plotted for each mutant of PLB (gray bars).

remained protected from labeling. Treatment of the proteoliposomes with detergent resulted in labeling of all molecules of PLB, where the ratio of labeled PLB in the absence and presence of detergent was used to calculate percent labeling (Figure 2). Biotin labeling prevents binding of the anti-phospholamban antibody, 2D12, so this was used to confirm that all molecules of PLB were biotinylated in detergent solution. As a further control, biotin labeling was performed on co-reconstituted proteoliposomes of SERCA with synthetic peptides. These peptides, designated Leu_9 and Leu_{12} (*22*), are helical transmembrane peptides comprised of leucine and alanine residues, and capped on each side of the membrane with two lysine residues. As expected, only half of the lysines in these co-reconstituted peptides were labeled in the absence of detergent (Figure 2, bottom panel, control), while the remaining lysines facing the interior of the proteoliposomes were protected from labeling. This same strategy was used for all PLB mutants described herein, as well as for those described in a previous publication (*20*). On average, 78 ± 1% of the PLB molecules were oriented with their cytoplasmic domains protruding from the outer surface of the proteoliposomes (n = 88, including the wild type and all mutants). Mutation of individual residues in the transmembrane domain had no effect on the reconstitution behavior or the orientation of PLB (for the sake of simplicity, the PLB mutants shown in Figure 2 are grouped according to PLB domain). Given that there are 4.5 molecules of PLB per molecule of SERCA in our co-reconstituted proteoliposomes (*20*), the data show that 3.6 molecules of PLB are correctly oriented relative to each SERCA molecule.

Effects of PLB Mutation on the Apparent Calcium Affinity of SERCA. Residues 34−52 of PLB (Figure 1) were mutated to alanine; each mutant was co-reconstituted with SERCA into proteoliposomes, and the calcium-dependent ATPase activity of SERCA in the co-reconstituted proteoliposomes was measured. This approach allowed us to test the ability of PLB mutants to alter the calcium affinity of SERCA in a chemically pure membrane environment (Table 1 and Figure 3). As an example of a loss-of-function PLB mutant, the Asn^{34}-to-Ala has been shown to alter the apparent calcium affinity of SERCA to a far lesser extent than wild-type PLB. The K_{Ca} values for SERCA alone, SERCA in the presence of wild-type PLB, and SERCA in the presence of N34A PLB were determined to be 0.41, 0.69, and 0.45 μM, respectively. As an example of a gain-of-function PLB mutant, Ile^{47}-to-Ala was shown to alter the apparent calcium affinity of SERCA to a far greater extent than wild-type PLB. The K_{Ca} value for SERCA in the presence of I47A PLB was determined to be 1.87 μM. Of the PLB mutants examined, two resulted in a loss of function (N34A and I38A), nine resulted in a gain of function (C36A, L37A, L39A, I40A, L43A, L44A, I47A, V49A, and L51A), and the remainder were considered neutral mutations. Losses or gains of function were defined as a statistically significant decrease or increase in the calcium affinity of SERCA compared to that of wild-type PLB. As in previous studies (*5*, *8*, *33*), we found that Asn^{34} and Ile^{38} were critical for PLB inhibitory function and that a majority of the gain-of-function mutants were clustered at the monomer−monomer interface of the PLB pentamer [residues at the **a**, **d**, and **g** positions (*9*, *34*)].

We also found differences in the behavior of some of the PLB mutants compared to previous studies (*5*, *8*, *33*). PLB mutants F35A, L42A, and I48A were originally found to result in severe losses of function, while mutants L39A and V49A were originally found to result in slight losses of function. Our results revealed

that F35A had no effect on PLB inhibitory function, L42A and I48A were slight loss-of-function mutants, and L39A and V49A were slight gain-of-function mutants. The differences between our studies and those previously reported by others (*5*, *8*, *33*) may be due to the human PLB protein utilized herein versus the canine PLB protein used in previous studies. However, this is difficult to rationalize with only two conservative residue changes between human and canine PLB. Glu^{2} and Lys^{27} are Asp^{2} and Asn^{27}, respectively, in the canine sequence. Nonetheless, the regulatory contributions of individual residues may be context-dependent, where the complex interaction of many residues ultimately leads to the modulation of SERCA calcium transport.

Effects of PLB Mutation on the Maximal Activity of SERCA. Our previous studies with co-reconstituted proteoliposomes indicated that PLB increased the maximal activity of SERCA, and that this behavior could be modulated by PLB mutation (*20*). Moreover, the ability to alter the calcium affinity of SERCA correlated with the ability to alter its maximal activity, and a similar trend was observed for peptide mimics of PLB (*19*, *22*). However, we currently lack an explanation for this phenomenon. To fully evaluate this behavior, we assessed the ability of all transmembrane mutants of PLB to alter the V_{max} of SERCA (Table 1 and Figure 4). The V_{max} value for SERCA in reconstituted proteoliposomes in the absence of PLB was 4.3 ± 0.1 μmol mg^{-1} min^{-1}. The V_{max} values for SERCA co-reconstituted in the presence of wild-type and mutant forms of PLB ranged from 4.0 to 6.0 μmol mg^{-1} min^{-1}. As previously described (*20*), a correlation was observed between the ability of the mutants to decrease the K_{Ca} and to increase the V_{max} of SERCA (not shown). In general, mutation of residues in the middle of the transmembrane domain (centered on residues 40−44) had a marginal impact on the ability of PLB to increase the V_{max} of SERCA, while mutation of residues at either end of the transmembrane domain had a significant impact (Figure 4).

The four residues that had the strongest effects on the ability of PLB to increase the V_{max} of SERCA were the N-terminal residues Asn^{34} and Leu^{37} and the C-terminal residues Met^{50} and Leu^{51}. In membranes, leucine and methionine are stronger helix promoters than alanine (*35*), while alanine is a much stronger helix promoter than asparagine. Thus, it is tempting to speculate that helical stability and/or flexibility plays a role in the interaction with SERCA. The proper helical structure or inherent flexibility at either end of the PLB transmembrane domain could play a role in correct protein−protein interactions. An insertion of an alanine at these positions could impact the tertiary and/or dynamic structure of PLB's transmembrane helix, thereby influencing the ability of PLB to alter the maximal activity of SERCA.

Effects of Mutation on the Cooperativity of SERCA. Our SERCA activity plots in the absence and presence of PLB mutants were fit to the Hill equation, where the Hill coefficient, n_H, provided a measure of the degree of cooperative ligand binding to SERCA. As before, the apparent n_H for SERCA reconstituted in the absence of PLB was 1.6 ± 0.1 ($n = 28$), while SERCA co-reconstituted with wild-type PLB yielded a value of 2.0 ± 0.1 ($n = 9$). The majority of the mutants had only a minimal effect on the ability of PLB to alter the cooperativity of SERCA (Table 1 and Figure 5). Three mutants, Phe^{35}, Leu^{39}, and Cys^{46}, caused the largest change in the Hill coefficient. While these mutants altered the K_{Ca} and V_{max} of SERCA to a level comparable to that of wild-type PLB, the increase in cooperativity normally observed with wild-type PLB was markedly reduced.

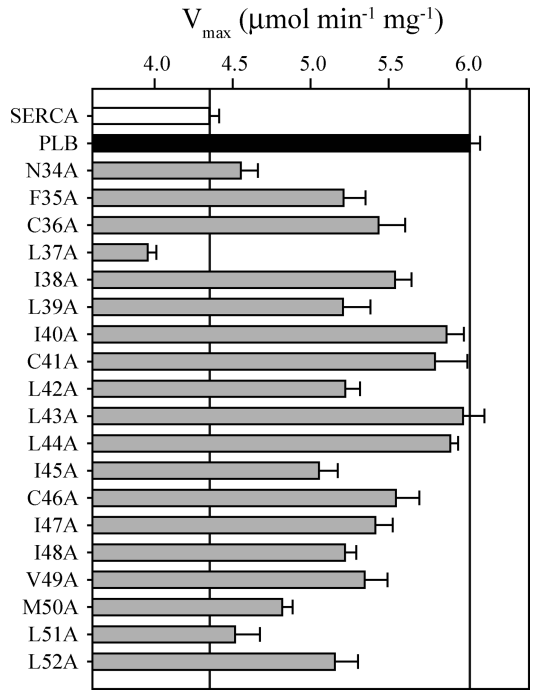

FIGURE 4: Effects of alanine mutation in the TM domain of PLB on the maximal activity (V_{max}) of SERCA. The vertical line at the left represents the V_{max} for SERCA reconstituted alone (white bar, $V_{max} = 4.3 \pm 0.1$ μmol mg^{-1} min^{-1}), and the vertical line at the right represents the V_{max} for SERCA co-reconstituted in the presence of wild-type PLB (black bar, $V_{max} = 6.0 \pm 0.1$ μmol mg^{-1} min^{-1}). The V_{max} values are plotted for each mutant of PLB (gray bars).

Kinetic Simulations. Equilibrium measurements of SERCA ATPase activity versus calcium concentration have been fit to a reaction equation based on two interacting calcium-binding sites (*16*, *17*). The reaction scheme assumes that calcium binding to SERCA occurs as highly cooperative steps linked by a conformation transition (Figure 1). In the model, calcium transport by SERCA has a slow conformational transition ($E \cdot Ca \leftrightarrow E' \cdot Ca$) that activates the enzyme by increasing the affinity for binding of a second calcium ion ($E' \cdot Ca \leftrightarrow E' \cdot CaCa$). PLB is thought to slow this conformational change, resulting in a reduction in the apparent calcium affinity of SERCA and increased cooperativity for calcium binding. Using kinetic simulations (*17*, *19*, *22*), we wished to improve our understanding of the experimentally observed shifts in the K_{Ca}, V_{max}, and n_H of SERCA in the presence of PLB (Figure 6). The SERCA ATPase activity curves in the absence or presence of each mutant were fit to the model of Cantilina et al. (*17*) using Dynafit (*30*). The best fit to the data was obtained by allowing rate constants for the first three steps in the reaction cycle to vary individually or in concert and minimizing the sum-of-squares error. The activity of SERCA in the absence of PLB was fit first, providing the starting point for optimization of the fit for SERCA co-reconstituted with PLB. Optimization of the $B_{forward}$ and $B_{reverse}$ rate constants alone (dotted line in Figure 6) did not provide an optimal fit, necessitating the inclusion of $C_{forward}$ in the fitting process (solid line in Figure 6).

In our standard analysis using Hill plots, each mutant could be classified as loss-of-function, neutral, or gain-of-function mutant compared to wild-type PLB. As a result, each mutant had a distinct effect on the K_{Ca}, V_{max}, and n_H of SERCA, such that a range of values was observed. The observed K_{Ca} values ranged from 0.41 to 1.87 μM calcium; the observed V_{max} values ranged

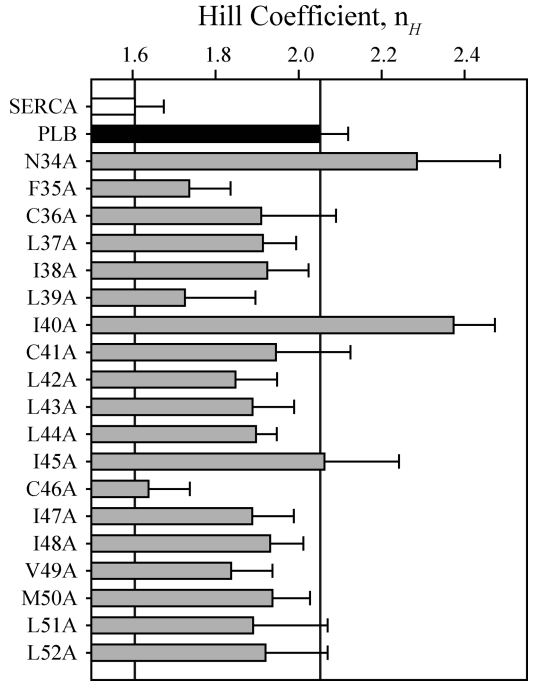

FIGURE 5: Effects of alanine mutation in the TM domain of PLB on the Hill coefficient (n_H) of SERCA. The vertical line at the left represents the n_H for SERCA reconstituted alone (white bar, n_H = 1.6 ± 0.1), and the vertical line at the right represents the n_H for SERCA co-reconstituted in the presence of wild-type PLB (black bar, n_H = 2.0 ± 0.1). The n_H values are plotted for each mutant of PLB (gray bars).

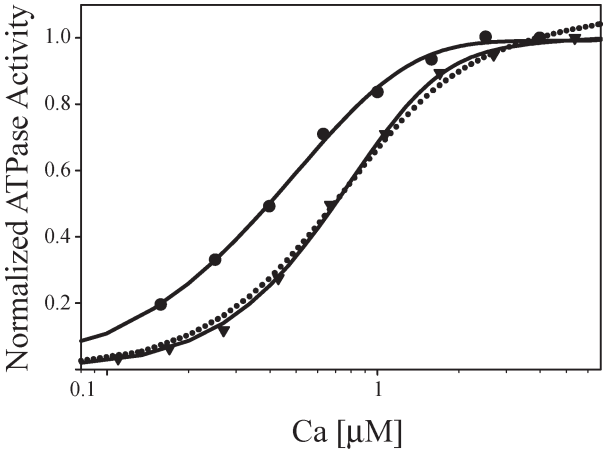

FIGURE 6: Kinetic simulations of SERCA ATPase activities. Normalized ATPase activities (V/V_{max}) of SERCA alone (●) or in the presence of wild-type PLB (▼) are plotted as a function of calcium concentration. The activity data in the graphs were fit using the reaction scheme of Cantilina (*17*) to minimize the sum-of-squares error. Best fits are shown as solid lines, and the rate constants obtained for the first three steps of the reaction cycle are listed in Table 2. For SERCA in the presence of wild-type PLB, the best fit (solid line) was obtained by altering the $C_{forward}$, $B_{forward}$, and $B_{reverse}$ rate constants (for the dotted line, only the $B_{forward}$ and $B_{reverse}$ constants were allowed to vary).

from 4.0 to 6.0 μmol mg^{-1} min^{-1}, and the Hill coefficients ranged from 1.6 to 2.4. Therefore, the changes in SERCA ATPase parameters induced by each PLB mutant (Table 1) could be examined for proportional changes in the kinetic parameters that result from the simulations (Table 2). As hypothesized, we could link the effects of PLB mutants on the calcium affinity, maximal activity, and cooperativity of SERCA to distinct steps in the reaction cycle.

Table 2: Rate Constants (s^{-1}) Resulting from the Kinetic Simulations[a]

	sum of squares[b]	$A_{forward}$	$A_{reverse}$	$B_{forward}$	$B_{reverse}$	$C_{forward}$	$C_{reverse}$
SERCA	0.003	216000	400	30	40	2567000	16
PLB	0.004	216000	400	44	50900	404000	16
N34A	0.003	290000	400	34	605	560000	16
F35A	0.008	120000	400	37	47700	1100000	16
C36A	0.006	110000	400	41	106000	560000	16
L37A	0.002	216000	400	29	36000	81100	16
I38A	0.009	216000	400	40	21000	928000	16
L39A	0.006	410000	400	47	490000	420000	16
I40A	0.01	210000	400	42	720	180000	16
C41A	0.020	216000	400	41	38000	270000	16
L42A	0.008	216000	400	38	108700	904000	16
L43A	0.008	216000	400	44	51500	130000	16
L44A	0.002	216000	400	44	81000	173000	16
I45A	0.009	260000	400	35	850	370000	16
C46A	0.005	120000	400	40	490000	5800000	16
I47A	0.005	57000	400	38	250	19000	16
I48A	0.003	300000	400	39	100000	370000	16
V49A	0.009	150000	400	38	86000	440000	16
M50A	0.0009	180000	400	34	22000	670000	16
L51A	0.007	110000	400	35	260000	780000	16
L52A	0.01	216000	400	37	61500	520000	16

[a]For kinetic anaylsis, the reaction scheme and initial rate constants were taken from ref *17* with the forward and reverse rate constants corresponding to the steps as depicted in Figure 1. [b]The final fits of the experimental data were chosen on the basis of minimization of the sum-of-squares error.

Kinetic Simulations versus K_{Ca}. As originally postulated (*17*), PLB mutants that altered the apparent calcium affinity of SERCA also increased the reverse rate constant for the isomeric transition following calcium binding [$B_{reverse}$ (Figure 1 and Table 2)]. Despite this observation, there was no correlation between the effect on K_{Ca} and $B_{reverse}$ (not shown). Instead, there was a clear relationship between the ability of the PLB mutants to alter K_{Ca} and the forward rate constant for binding of the second calcium ion ($C_{forward}$). We observed an exponential decay in $C_{forward}$ as K_{Ca} increased (Figure 7), such that PLB mutants that decreased the apparent calcium affinity of SERCA resulted in a proportional decrease in the forward rate of binding of the second calcium ion. Therefore, PLB inhibition appeared to drive the reaction (E + Ca ↔ E·Ca ↔ E′·Ca ↔ E′·Ca + Ca ↔ E′·CaCa) toward the E·Ca state of SERCA by altering two steps in the reaction scheme, namely, by increasing $B_{reverse}$ (E·Ca ← E′·Ca) and decreasing $C_{forward}$ (E′·Ca ← E′·CaCa) (Figure 1).

There are two notable exceptions. First, the C46A mutant did not significantly change K_{Ca} compared to that of wild-type PLB, yet it affected both $C_{forward}$ ($C_{forward}$ increased 14-fold compared to that of wild-type PLB) and $B_{reverse}$ ($B_{reverse}$ increased 10-fold compared to that of wild-type PLB). The increase in $C_{forward}$ overcomes the effect on $B_{reverse}$, such that a wild-type-like effect on K_{Ca} is observed; however, there is a loss of cooperativity compared to that of wild-type PLB. Second, I47A was the largest gain-of-function mutant, yet there was a minimal effect on $B_{reverse}$ (compared to SERCA alone). Instead, the values of $A_{forward}$ and $C_{forward}$ were among the lowest observed, suggesting that this mutant uses a distinct mechanism to alter the calcium affinity of SERCA. Rather than altering the conformational transition following calcium binding, this PLB mutant suppressed the binding of both the first and second calcium ions.

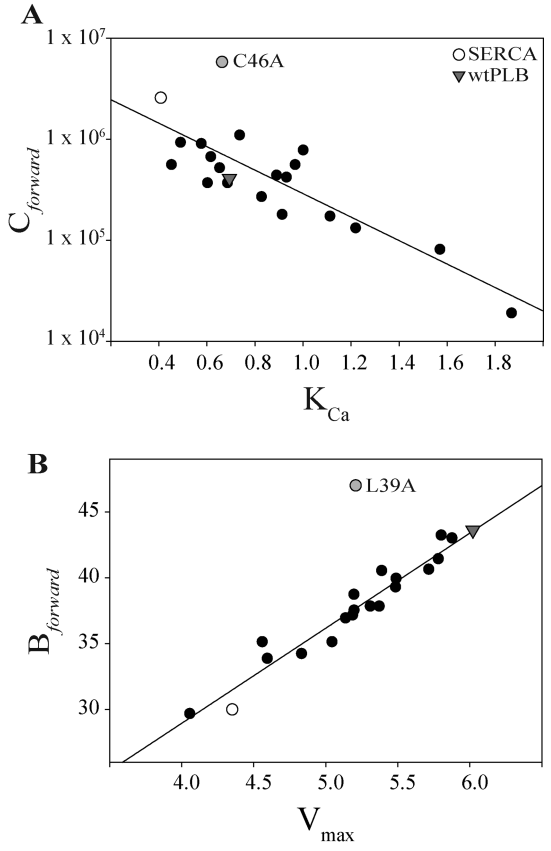

FIGURE 7: Correlations between the rate constants in the kinetic simulations and the calcium affinity (A) and maximal activity (B) of SERCA in the presence of PLB mutants. The value for SERCA alone is shown as an empty circle, while the value for SERCA in the presence of wild-type PLB is indicated as a gray triangle. (A) C_{forward} rate constant from the kinetic simulations plotted vs K_{Ca} for each mutant. The data were fit by linear regression ($R^2 = 0.66$). C46A (gray circle) deviated significantly from this correlation. (B) B_{forward} rate constant from the kinetic simulations plotted vs V_{max} for each mutant. The data were fit by linear regression ($R^2 = 0.93$). The L39A mutant alone (gray circle) did not show this same correlation.

Kinetic Simulations versus V_{max}. The effect of PLB on the maximal activity of SERCA has been controversial (*36*−*39*), though the use of reconstitution systems has demonstrated that this effect is reproducible and sensitive to PLB mutation (*20*, *33*). The kinetic simulations provide an explanation for the ability of PLB to increase the maximal activity of SERCA. As originally demonstrated by Inesi and colleagues (*17*), PLB appeared to alter both the forward and reverse rate constants for the isomeric transition following calcium binding, where the latter rate constant accounted for the change in the apparent calcium affinity of SERCA. We have observed a clear relationship between the ability of the PLB mutants to alter V_{max} and the forward rate constant for binding of the first calcium ion [B_{forward} (Figure 7)]. The L39A mutant is the one notable exception. Nonetheless, this suggests that accelerating the formation of E′·Ca (by increasing B_{forward}) increases the turnover rate and maximal activity of the enzyme.

DISCUSSION

Apparent Calcium Affinity of SERCA. There have been numerous studies examining the effects of PLB mutation on the functional interaction with SERCA (*2*−*8*, *20*, *33*, *40*−*42*). Combined with a variety of other biochemical data, including cross-linking constraints, several congruent molecular models have been proposed (*10*−*13*, *43*, *44*). The transmembrane domain of PLB is largely responsible for the inhibitory interaction, which manifests itself as a change in the apparent calcium affinity of SERCA. One face of PLB's transmembrane helix is responsible for the physical interaction with SERCA, where a handful of residues have been shown to be essential for inhibitory function. For instance, Asn^{34} is an essential residue that is proposed to form a hydrogen bond with Thr^{317} and/or Thr^{805} (*13*, *19*). The opposite face of PLB's transmembrane helix, composed of leucine and isoleucine residues, is responsible for self-association and stabilization of a homopentameric state, where mutation of these residues results in superinhibition of SERCA. This was originally presumed to result from an increase in the amount of PLB monomer [the so-called "mass action" theory (*5*)]. However, current models suggest that residues around the entire circumference of the PLB transmembrane domain contribute to the interaction with SERCA, including the leucine-isoleucine zipper residues (*8*, *13*).

Despite this wealth of detail, few attempts have been made to reconcile the mutagenesis data with the original observation on the mechanism of SERCA inhibition by PLB, namely, that PLB alters the slow isomeric transition following binding of the first calcium ion (*17*). In the original study, a monoclonal antibody against PLB was used to reverse inhibition in steady-state and kinetic measurements of calcium activation in a cardiac SR vesicle preparation (comparisons were also made to skeletal SR vesicles). PLB specifically altered the forward and reverse rate constants for a structural transition following binding of calcium to SERCA. Herein, we wished to systematically vary the inhibitory activity of PLB, thereby varying the apparent calcium affinity, maximal activity, and cooperativity of SERCA. This was achieved using scanning-alanine mutagenesis of the transmembrane domain of recombinant PLB followed by co-reconstitution with SERCA into proteoliposomes (*20*). We could then perform kinetic simulation of our ATPase activity isotherms using the previously established reaction scheme (*16*). The hypothesis was that varying the apparent calcium affinity of SERCA through PLB mutation should result in a proportional change in one or more of the rate constants in the SERCA reaction scheme (presumably B_{forward} and B_{reverse}, as originally postulated).

Scanning-alanine mutagenesis of the transmembrane domain of PLB allowed modulation of SERCA inhibition over a wide range of apparent calcium affinities. The measured calcium affinity of SERCA varied from 0.45 μM in the presence of the loss-of-function mutant N34A to 1.87 μM in the presence of the gain-of-function mutant I47A (Table 1). Kinetic simulation for all 19 PLB mutants revealed changes in the reaction rate constants for the first three steps in the transport cycle. First, all PLB mutants altered B_{reverse}, the reverse rate constant for a slow isomeric transition in SERCA following binding of the first calcium ion. While this was consistent with prior observations (*17*), there was no clear relationship between B_{reverse} and the shift in the apparent calcium affinity of SERCA. For instance, the two gain-of-function mutants, L37A and I47A, had similar effects on SERCA (K_{Ca} values of 1.57 ± 0.04 and 1.87 ± 0.07 μM, respectively), yet they had markedly different effects on B_{reverse} (compared to a value of 40 s^{-1} for SERCA in the absence of PLB, values of 36000 and 250 s^{-1} were obtained, respectively). Second, all PLB mutants also altered C_{forward}, the forward rate constant for binding of a second calcium ion to SERCA. In this case, there was a clear correlation between

$C_{forward}$ and the shift in the apparent calcium affinity of SERCA. For instance, the two gain-of-function mutants, L37A and I47A, had a similar effect on SERCA, and this was reflected in their similar effects on $C_{forward}$ (compared to a value of 2567000 s^{-1} for SERCA in the absence of PLB, low values of 81100 and 19000 s^{-1} were obtained, respectively). This decrease in the binding rate of the second calcium ion may play a significant role in the increased inhibitory activity of these two gain-of-function mutants. For the I47A mutant, the decreased rate of binding of the second calcium ion is accompanied by a 75% reduction in the rate of binding of the first calcium ion as well, making this mutant the largest supershifter we have characterized.

On average, the PLB mutants caused an approximately 1000-fold decrease in the equilibrium constant for formation of the E′·Ca state and an approximately 6-fold decrease in the equilibrium constant for formation of the E′·CaCa state. Surprisingly, it is this latter effect that correlated more strongly with the ability of PLB to shift the apparent calcium affinity of SERCA. Nonetheless, a subset of mutants deviated from this behavior. Two of these mutants will be discussed here: alanine substitution of Leu^{37} and Ile^{47}. Mutation of Leu^{37} resulted in a supershifter that also depressed the V_{max} of SERCA, and this correlated with suppression of the E·Ca → E′·Ca and E′·Ca + Ca → E′·CaCa transitions. In structural models, Leu^{37} has been suggested to interact with Leu^{797} on transmembrane segment M6 of SERCA (*13*). Mutation of Ile^{47} resulted in the largest supershifter that we observed. However, this mutant had a minimal effect on the E·Ca ↔ E′·Ca transition, suggesting that it should be a loss-of-function form of PLB. The kinetic simulations demonstrate that the potent inhibition of this mutant is due to major changes in the E + Ca → E·Ca and E′·Ca + Ca → E′·CaCa transitions of SERCA. In current molecular models, Ile^{47} is not predicted to interact with SERCA (*10*, *13*, *15*). Nonetheless, this residue is proximal to the luminal ends of M2 and M9 of SERCA, and it has been demonstrated that this residue can be cross-linked to M2 (*10*).

Each of the residues mentioned above had a distinct effect on SERCA activity that correlated with individual steps in the kinetic simulations of calcium transport. These observations are supported by the unique sets of interactions with SERCA postulated for each residue, emphasizing the subtlety and complexity of the interaction between these two proteins. The rearrangement of transmembrane helices M1−M6 of SERCA during the calcium transport cycle (E2 to E1 transition) allows residues to alternately participate in the liganding sphere of the calcium ions that bind to sites I and II of SERCA in a conformation-dependent manner. The binding site for the PLB monomer is formed by transmembrane segments M2, M4, M6, and M9 of SERCA. Calcium binding to site I involves Thr^{799} and Asp^{800} of M6, and calcium binding to site II involves Asn^{796} of M6. Since calcium binding to site I initiates cooperative binding to site II, PLB is well positioned to alter the interaction and occupancy of both calcium binding sites. Therefore, subtle changes in the interaction between PLB and SERCA in this region can impact not only the apparent calcium affinity of SERCA but also the maximal activity and cooperativity.

Maximal Activity of SERCA. In this study, none of the transmembrane mutants had a greater effect on V_{max} than wild-type PLB, and only one mutant, L37A, actually decreased the V_{max} from that evidenced by SERCA alone. In kinetic simulations, this effect on V_{max} correlated well with the $B_{forward}$ rate constant (E·Ca → E′·Ca). At subsaturating calcium concentrations, the effect on $B_{reverse}$ dominates and manifests itself as a change in the apparent calcium affinity of SERCA (E·Ca ← E′·Ca). However, at saturating calcium concentrations, the effect on $B_{forward}$ dominates and manifests itself as a change in the maximal activity of SERCA (E·Ca → E′·Ca). This serves to emphasize the subtle effect that the transmembrane mutations have on the conformation of PLB and SERCA such that the apparent calcium affinity and maximal velocity of the enzyme can be altered. The L39A mutant of PLB was the only one that deviated from this behavior. In our kinetic simulations, it caused a disproportionate increase in the (E·Ca → E′·Ca) transition compared to its ability to stimulate V_{max} of SERCA. In the structural models of the SERCA−PLB complex, this residue aligns with Trp^{794} on M6 and Leu^{943} and Leu^{946} on M9 of SERCA (*15*).

The molar ratio of SERCA and PLB used in these studies mimics that of cardiac SR (*45*), suggesting that the effects that we have observed on the V_{max} of SERCA may occur under physiological conditions. However, this point remains controversial. The co-reconstitution method used here has consistently revealed that PLB increases the V_{max} of SERCA (*20*, *22*, *33*), while an alternative method of co-reconstitution has demonstrated that PLB decreases the V_{max} of SERCA (*36*). Studies in cardiac SR or coexpression systems have shown that PLB decreases (*37*−*39*, *46*) or has no effect (*47*−*49*) on the V_{max} of SERCA. Nonetheless, as demonstrated using the co-reconstitution method described herein, the increase in the V_{max} of SERCA can be reversed by either mutation of PLB (*20*, *33*) or reduction of the PLB:SERCA molar stoichiometry (*22*, *33*). In our hands, however, the increase in the V_{max} of SERCA is not reversed by either phosphorylation of PLB at Ser^{16} (*20*) or treatment with an anti-PLB monoclonal antibody (data not shown).

There are many potential explanations for the observation that the co-reconstitution method used herein consistently yields an increase in the V_{max} of SERCA. For instance, in the presence of PLB, SERCA may be better protected from inactivation during the co-reconstitution procedure. Indeed, it is clear that the specific activity of SERCA can be impacted by the choice of lipid and detergent used in the reconstitution, as well as the sequence of the regulatory peptide (*19*, *20*, *22*, *33*, *36*, *50*). However, we are compelled to consider other possibilities, given that the effect on the SERCA maximal activity can be reversed either by mutation of PLB or by lowering the stoichiometry. In this study, we conclude that PLB increases the V_{max} of SERCA by affecting a particular step in the calcium transport cycle. Therefore, this raises the possibility that SERCA function may be modulated by the amount of PLB present in the cardiac SR membrane, as originally suggested by Thomas and colleagues (*33*). While purely hypothetical, this would be an interesting adaptation under pathological conditions, where SERCA down-regulation during heart failure (*51*) could be partially offset by PLB-mediated activation.

ACKNOWLEDGMENT

We thank Jennifer Douglas and Shuo Chen for technical assistance.

REFERENCES

1. Kirchberger, M., Tada, M., and Katz, A. (1975) Phospholamban: A regulatory protein of the cardiac sarcoplasmic reticulum. *Recent Adv. Stud. Card. Struct. Metab. 5*, 103–115.

2. Kimura, Y., Kurzydlowski, K., Tada, M., and MacLennan, D. H. (1996) Phospholamban regulates the Ca^{2+}-ATPase through intramembrane interactions. *J. Biol. Chem. 271*, 21726–21731.
3. Kimura, Y., Asahi, M., Kurzydlowski, K., Tada, M., and MacLennan, D. (1998) Amino acids Lys-Asp-Asp-Lys-Pro-Val402 in the Ca^{2+}-ATPase of cardiac sarcoplasmic reticulum are critical for functional association with phospholamban. *J. Biol. Chem. 273*, 14238–14241.
4. Kimura, Y., Asahi, M., Kurzydlowski, K., Tada, M., and MacLennan, D. H. (1998) Phospholamban domain Ib mutations influence functional interactions with the Ca^{2+}-ATPase isoform of cardiac sarcoplasmic reticulum. *J. Biol. Chem. 273*, 14238–14241.
5. Kimura, Y., Kurzydlowski, K., Tada, M., and MacLennan, D. H. (1997) Phospholamban inhibitory function is enhanced by depolymerization. *J. Biol. Chem. 272*, 15061–15064.
6. Asahi, M., Kimura, Y., Kurzydlowski, K., Tada, M., and MacLennan, D. (1999) Transmembrane helix M6 in sarco(endo)plasmic reticulum Ca^{2+}-ATPase forms a functional interaction site with phospholamban. Evidence for physical interactions at other sites. *J. Biol. Chem. 274*, 32855–32862.
7. Autry, J., and Jones, L. (1997) Functional co-expression of the canine cardiac Ca^{2+} pump and phospholamban in *Spodoptera frugiperda* (Sf21) cells reveals new insights on ATPase regulation. *J. Biol. Chem. 272*, 15872–15880.
8. Cornea, R., Autry, J., Chen, Z., and Jones, L. (2000) Re-examination of the role of the leucine/isoleucine zipper residues of phospholamban in inhibition of the Ca^{2+}-pump of cardiac sarcoplasmic reticulum. *J. Biol. Chem. 275*, 41487–41494.
9. Simmerman, H., Kobayashi, Y., Autry, J., and Jones, L. (1996) A leucine zipper stabilizes the pentameric membrane domain of phospholamban and forms a coiled-coil pore structure. *J. Biol. Chem. 271*, 5941–5946.
10. Chen, Z., Akin, B., Stokes, D., and Jones, L. (2006) Cross-linking of C-terminal residues of phospholamban to the Ca^{2+} pump of cardiac sarcoplasmic reticulum to probe spatial and functional interactions within the transmembrane domain. *J. Biol. Chem. 281*, 14163–14172.
11. Chen, Z., Stokes, D., and Jones, L. (2005) Role of leucine 31 of phospholamban in structural and functional interactions with the Ca^{2+} pump of cardiac sarcoplasmic reticulum. *J. Biol. Chem. 280*, 10530–10539.
12. Chen, Z., Stokes, D., Rice, W., and Jones, L. (2003) Spatial and dynamic interactions between phospholamban and the canine cardiac Ca^{2+} pump revealed with use of heterobifunctional cross-linking agents. *J. Biol. Chem. 278*, 48348–48356.
13. Toyoshima, C., Asahi, M., Sugita, Y., Khanna, R., Tsuda, T., and MacLennan, D. (2003) Modeling of the inhibitory interaction of phospholamban with the Ca^{2+} ATPase. *Proc. Natl. Acad. Sci. U.S.A. 100*, 467–472.
14. Morita, T., Hussain, D., Asahi, M., Tsuda, T., Kurzydlowski, K., Toyoshima, C., and Maclennan, D. H. (2008) Interaction sites among phospholamban, sarcolipin, and the sarco(endo)plasmic reticulum Ca^{2+}-ATPase. *Biochem. Biophys. Res. Commun. 369*, 188–194.
15. Seidel, K., Andronesi, O. C., Krebs, J., Griesinger, C., Young, H. S., Becker, S., and Baldus, M. (2008) Structural Characterization of Ca^{2+}-ATPase-Bound Phospholamban in Lipid Bilayers by Solid-State Nuclear Magnetic Resonance (NMR) Spectroscopy. *Biochemistry 47*, 4369–4376.
16. Inesi, G., Kurzmack, M., and Lewis, D. (1988) Kinetic and equilibrium characterization of an energy-transducing enzyme and its partial reactions. *Methods Enzymol. 157*, 154–190.
17. Cantilina, T., Sagara, Y., Inesi, G., and Jones, L. R. (1993) Comparative studies of cardiac and skeletal sarcoplasmic reticulum ATPases: Effect of phospholamban antibody on enzyme activation. *J. Biol. Chem. 268*, 17018–17025.
18. Waggoner, J. R., Huffman, J., Froehlich, J. P., and Mahaney, J. E. (2007) Phospholamban inhibits Ca-ATPase conformational changes involving the E2 intermediate. *Biochemistry 46*, 1999–2009.
19. Afara, M., Trieber, C., and Young, H. (2008) Peptide inhibitors use two related mechanims to alter the apparent calcium affinity of the sarcoplasmic reticulum calcium pump. *Biochemistry 47*, 2522–2530.
20. Trieber, C., Douglas, J., Afara, M., and Young, H. (2005) The effects of mutation on the regulatory properties of phospholamban in co-reconstituted membranes. *Biochemistry 44*, 3289–3297.
21. Douglas, J., Trieber, C., Afara, M., and Young, H. (2005) Rapid, high-yield expression and purification of Ca^{2+}-ATPase regulatory proteins for high-resolution structural studies. *Protein Expression Purif. 40*, 118–125.
22. Afara, M., Trieber, C., Glaves, J., and Young, H. (2006) Rational design of peptide inhibitors of the sarcoplasmic reticulum calcium pump. *Biochemistry 45*, 8617–8627.
23. Warren, G. B., Toon, P. A., Birdsall, N. J. M., Lee, A. G., and Metcalfe, J. C. (1974) Reconstitution of a calcium pump using defined membrane components. *Proc. Natl. Acad. Sci. U.S.A. 71*, 622–626.
24. Eletr, S., and Inesi, G. (1972) Phospholipid orientation in sarcoplasmic reticulum membranes: Spin-label ESR and proton NMR studies. *Biochim. Biophys. Acta 282*, 174–179.
25. Stokes, D. L., and Green, N. M. (1990) Three-dimensional crystals of Ca-ATPase from sarcoplasmic reticulum: Symmetry and molecular packing. *Biophys. J. 57*, 1–14.
26. Reddy, L. G., Jones, L. R., Cala, S. E., O'Brian, J. J., Tatulian, S. A., and Stokes, D. L. (1995) Functional reconstitution of recombinant phospholamban with rabbit skeletal Ca-ATPase. *J. Biol. Chem. 270*, 9390–9397.
27. Young, H. S., Rigaud, J. L., Lacapere, J. J., Reddy, L. G., and Stokes, D. L. (1997) How to make tubular crystals by reconstitution of detergent-solubilized Ca^{2+}-ATPase. *Biophys. J. 72*, 2545–2558.
28. Young, H., Reddy, L., Jones, L., and Stokes, D. (1998) Co-reconstitution and co-crystallization of phospholamban and Ca^{2+}-ATPase. *Ann. N.Y. Acad. Sci. 853*, 103–115.
29. Young, H. S., Jones, L. R., and Stokes, D. L. (2001) Locating phospholamban in co-crystals with Ca^{2+}-ATPase by cryoelectron microscopy. *Biophys. J. 81*, 884–894.
30. Kuzmic, P. (1996) Program DYNAFIT for the analysis of enzyme kinetic data: Application to HIV proteinase. *Anal. Biochem. 237*, 260–273.
31. Stokes, D., Pomfret, A., Rice, W., Glaves, J., and Young, H. (2006) Interactions between Ca^{2+}-ATPase and the pentameric form of phospholamban in two-dimensional co-crystals. *Biophys. J. 90*, 4213–4223.
32. Levy, D., Gulik, A., Bluzat, A., and Rigaud, J.-L. (1992) Reconstitution of the sarcoplasmic reticulum Ca^{+2}-ATPase: Mechanisms of membrane protein insertion into liposomes during reconstitution procedures involving detergents. *Biochim. Biophys. Acta 1107*, 283–298.
33. Reddy, L., Cornea, R., Winters, D., McKenna, E., and Thomas, D. (2003) Defining the molecular components of calcium transport regulation in a reconstituted membrane system. *Biochemistry 42*, 4585–4592.
34. Oxenoid, K., and Chou, J. (2005) The structure of phospholamban pentamer reveals a channel-like architecture in membranes. *Proc. Natl. Acad. Sci. U.S.A. 102*, 10870–10875.
35. Liu, L. P., and Deber, C. M. (1998) Uncoupling hydrophobicity and helicity in transmembrane segments. α-Helical propensities of the amino acids in non-polar environments. *J. Biol. Chem. 273*, 23645–23648.
36. Hughes, G., Starling, A., Sharma, R., East, J., and Lee, A. (1996) An investigation of the mechanism of inhibition of the Ca^{2+}-ATPase by phospholamban. *Biochem. J. 318*, 973–979.
37. Sasaki, T., Inui, M., Kimura, Y., Kuzuyu, T., and Tada, M. (1992) Molecular mechanism of regulation of Ca^{2+} pump ATPase by phospholamban in cardiac sarcoplasmic reticulum. *J. Biol. Chem. 267*, 1674–1679.
38. Antipenko, A., Spielman, A., and Kirchberger, M. (1997) Comparison of the effects of phospholamban and jasmone on the calcium pump of cardiac sarcoplasmic reticulum. Evidence for modulation by phospholamban of both Ca^{2+} affinity and Vmax (Ca) of calcium transport. *J. Biol. Chem. 272*, 2852–2860.
39. Antipenko, A., Spielman, A., Sassaroli, M., and Kirchberger, M. (1997) Comparison of the kinetic effects of phospholamban phosphorylation and anti-phospholamban monoclonal antibody on the calcium pump in purified cardiac sarcoplasmic reticulum membranes. *Biochemistry 36*, 12903–12910.
40. Reddy, L., Autry, J., Jones, L., and Thomas, D. (1999) Co-reconstitution of phospholamban mutants with the Ca-ATPase reveals dependence of inhibitory function on phospholamban structure. *J. Biol. Chem. 274*, 7649–7655.
41. Asahi, M., Green, N., Kurzydlowski, K., Tada, M., and MacLennan, D. (2001) Phospholamban domain Ib forms an interaction site with the loop between transmembrane helices M6 and M7 of sarco-(endo)plasmic reticulum Ca^{2+}-ATPases. *Proc. Natl. Acad. Sci. U.S.A. 98*, 10061–10066.
42. Asahi, M., McKenna, E., Kurzydlowski, K., Tada, M., and MacLennan, D. (2000) Physical interactions between phospholamban and sarco-(endo)plasmic reticulum Ca^{2+}-ATPases are dissociated by elevated Ca^{2+}, but not by phospholamban phosphorylation, vanadate, or thapsigargin, and are enhanced by ATP. *J. Biol. Chem. 275*, 15034–15038.
43. Hutter, M., Krebs, J., Meiler, J., Griesinger, C., Carafoli, E., and Helms, V. (2002) A structural model of the complex formed by

phospholamban and the calcium pump of sarcoplasmic reticulum obtained by molecular mechanics. *ChemBioChem 3*, 1200–1208.
44. Chen, L., Yao, Q., Soares, T., Squier, T., and Bigelow, D. (2009) Phospholamban Modulates the Functional Coupling between Nucleotide Domains in Ca-ATPase Oligomeric Complexes in Cardiac Sarcoplasmic Reticulum. *Biochemistry 48*, 2411–2421.
45. Ferrington, D., Yao, Q., Squier, T., and Bigelow, D. (2002) Comparable levels of Ca-ATPase inhibition by phospholamban in slow-twitch skeletal and cardiac sarcoplasmic reticulum. *Biochemistry 41*, 13289–13296.
46. Antipenko, A., Spielman, A. I., and Kirchberger, M. A. (1999) Kinetic differences in the phospholamban-regulated calcium pump when studied in crude and purified cardiac sarcoplasmic reticulum vesicles. *J. Membr. Biol. 167*, 257–265.
47. Simmerman, H. K., and Jones, L. R. (1998) Phospholamban: Protein structure, mechanism of action, and role in cardiac function. *Physiol. Rev. 78*, 921–947.
48. Odermatt, A., Kurzydlowski, K., and MacLennan, D. H. (1996) The v_{max} of the Ca^{2+}-ATPase of cardiac sarcoplasmic reticulum (SERCA2a) is not altered by Ca^{2+}/calmodulin-dependent phosphorylation or by interaction with phospholamban. *J. Biol. Chem. 271*, 14206–14213.
49. Mahaney, J. E., Autry, J. M., and Jones, L. R. (2000) Kinetics studies of the cardiac Ca-ATPase expressed in Sf21 cells: New insights on Ca-ATPase regulation by phospholamban. *Biophys. J. 78*, 1306–1323.
50. Coll, R. J., and Murphy, A. J. (1984) Purification of the CaATPase of sarcoplasmic reticulum by affinity chromatography. *J. Biol. Chem. 259*, 14249–14254.
51. Hasenfuss, G., Reinecke, H., Studer, R., Pieske, B., Meyer, M., Drexler, H., and Just, H. (1996) Calcium cycling proteins and force-frequency relationship in heart failure. *Basic Res. Cardiol. 91* (Suppl. 2), 17–22.